Noname manuscript No.
(will be inserted by the editor)

All-round suppression of Cu_6Sn_5 growth in Sn/Cu joints by utilizing TiO_2 nanoparticles

Shengyan Shang [1] · **Anil Kunwar**[2] · **Jinye Yao** [1] · **Yunpeng Wang**[1] · **Ning Zhao**[1] · **Mingliang Huang**[1] · **Haitao Ma**[1,*]

Received: date / Accepted: date

Abstract Both TiO_2 and Cu nanoparticles, when added at the interface of the Sn/Cu joints during reflow soldering at 250 ℃ for 10, 60, 120 s and subsequent air cooling, are observed to reduce the growth of Cu_6Sn_5 whiskers. Though both reinforcments reduce the vertical growth of intermetallic compound (IMC), only TiO_2 could suppress the lateral growth of the compound. The solder saturation level with Cu at different reflow duration can influence final dimensions as well as morphology of IMC and occurrence of screw dislocation. The addition of TiO_2, by intervening the mechanism of ostwald ripening during reflow can be utilized to enhance the solder-IMC bonding at interface.

Keywords intermetallics · Diffusion · Crystal growth · Microstructure · Finite element modeling

1 Introduction

In microelectronic packaging sectors, the miniaturization trend of electronic devices and the utilization of fine pitch interconnections3, have highlighted the requirement of strong and reliable Pb-free solder joints. Interfacial Cu_6Sn_5 intermetallic compound (IMC), characterized by inherent brittle properties,

S.Y. Shang, J. Yao, Y. Wang, N. Zhao, H.T. Ma
[1]School of Materials Science and Engineering, Dalian University of Technology, 116024, Dalian, China

A. Kunwar
[2]School of Mechanical Engineering, Dalian University of Technology, 116024, Dalian, China

*Corrresponding Author
E-mail: htma@dlut.edu.cn (Haitao Ma)
Tel.: +86-0411-84707636
Fax: +86-0411-84707636

plays a vital role in determining overall solder joints strength. There is a broad consensus in the scientific community that solder joint properties could be enhanced by suppressing the interfacial Cu_6Sn_5 IMC layer[1,2,3,4]. Among several techniques, use of nanoparticles can be seen as a promising way to inhibit the growth of IMC in Sn based solders. The experiments regarding the influence of metallic and TiO_2 nanoparticles on the IMC heightwise thickness has been discussed in [1],[5],[6], but these works have not included the effect on the radial (widthwise) growth of IMC. The diffusion flux of Cu due to the difference in radii of curvature of Cu_6Sn_5 has a significant contribution in the annexation of adjacent IMC grains [7] and thus the investigation on the radial dimensions of IMC as influenced by nanoparticles, can provide some insight into this area.

The crystal growth mechanisms of primary Cu_6Sn_5 IMC in Sn-xCu alloys have been experimentally assessed by Xian et al [8], wherein it has been highlighted that cooling rate and Cu content affect the resulting morphology. So, the addition of nanoparticles, by influencing the supply rate of Cu at the ledge of growing crystal [9], can alter the rate of the screw dislocation driven growth of Cu_6Sn_5 and determine the overall growth kinetics of IMC. In this present study, Cu and TiO_2 nanoparticles of several weight proportions to solder flux, are added to the Sn solder and their effect on the growth behavior of IMC at the interface of Sn/Cu joints is discussed.

2 Materials and Methods

Cu nanoparticles were prepared by chemical reduction method schematically illustrated in Fig. 1 [10], which is explain clearly in our previous work [11]. TiO_2 were obtained from Haoxi Research Nanomaterials Inc., Shanghai, China. The morphology of these nanoparticles was characterized by the field emission scanning electron microscopy (NOVA Nano-SEM 450) as shown in Fig. 2(a) and Fig. 2(c). In the X-ray diffraction patterns of Fig. 2(b) and Fig. 2(d) obtained from X-ray diffractometer (XRD-6000) for the as-prepared Cu and purchased TiO_2 nanoparticles ; the peaks are very close to those reported in the Joint Committee on Powder Diffraction Standards (JCPDS), copper file No.04-0836 and TiO_2 file No.89-4921. These XRD peaks suggest that both materials are crystalline nanoparticles. From Scherrer's formula and full-width at half maximum (FWHM) data [12], the mean crystallite size of Cu and TiO_2 nanoparticles were obtained as 50 $\pm$ 5 nm and 44 $\pm$ 8 nm respectively.

In order to perform soldering reflow experiments, lead-free pure Sn solder balls of initial diameter of 1400 μm were used in this study. Cu and TiO_2 nanoparticles (NPs), each constituting 1 wt.% of original rosin flux (AMTECH:NC-559-ASM) were separately doped into the flux utilizing the methodogy described in [13]. Pure Cu sheets in dimensions of 15 mm $\times$ 5 mm $\times$ 100 μm were employed as substrates and cleaned in 5% HCl solution (vol.%) under the action of ultrasonic vibration. Pure rosin flux, Cu NPs + rosin flux and TiO_2 NPs + rosin flux, were applied at the interface of Sn solder and Cu

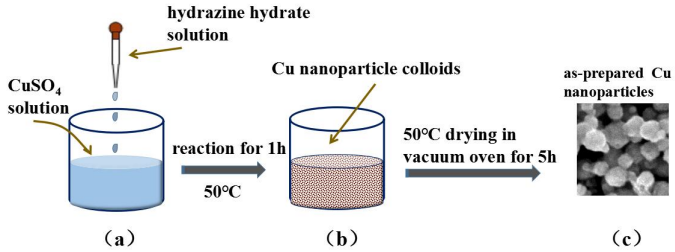

Fig. 1 Schematic sketch for preparation of Cu nanoparticles via chemical reduction method.

substrate; and this was followed by soldering reflow inside reflow oven (Forced Convection, FT02) at 250 ℃ for time durations of 10 , 60 and 120 s. During reflow heating, the NPs would disperse towards the molten solder bulk at the vicinity of interface and thus the samples are named as Sn, Sn + Cu NPs and Sn +TiO_2. After soldering, the samples were subjected to air cooling .Then, in order to show the top-view of solder joint, the joints were deep etched in nitric acid solution (10 vol.%) and followed ultrasonically cleaning by ethanol. For obtaining cross-sectional images, 5% HNO_3 + 2% HCl + 93% C_2H_5OH (in volume) solution was utilized to samples surface treat. The top-view and cross-sectional morphologies of the joints were observed by field emission scanning electron microscopy (Zeiss Supra 55 FESEM).

3 Results and Discussions

The cross sectional micrographs of Sn/Cu, Sn + Cu NPs/Cu and Sn +TiO_2/Cu joints are shown in Fig. 3. With the increase of reflow time duration, the Cu_6Sn_5 tend to grow as elongated prismatic whiskers in case of Sn/Cu system Fig. 3(a1)-(c1). The whiskering effect is slightly reduced in case of Sn + Cu NPs system (Fig. 3(a2)-(c2)) whereas whiskers are strongly suppressed by the solder with TiO_2 doped flux (Fig. 3(a3)-(c3)). Moreover, the IMCs are observed to grow with unform gap between them in case of Sn + TiO_2 samples.

Fig. 4 shows the top-view images of intermetallics compounds at the interface of the solder joints. As shown in Fig. 4(a1, a2, a3), the IMCs corresponding to the reflow duration of 10 s are characterized by the absence of distinct faceted planes whereas Cu_6Sn_5 IMC grains represented by Fig. 4(b1-b3,c1-c3) that correspond to reflow time of 60 and 120 s bear obviously observable faceted planes. This can be explained by the finite element method (FEM) based numerical simulation , presented in Fig. 5, for transient concentration distribution of Cu in the Sn solder balls (diameter = 1.4 mm) at T = 250 ℃. In accordance to the FEM results, the Sn solder processed at reflow duration of t =10 s, is not saturated with Cu and thus the precipitation driven growth of prismatic IMCs at interface is suppressed. In case of reflow for t= 60s, 120s;

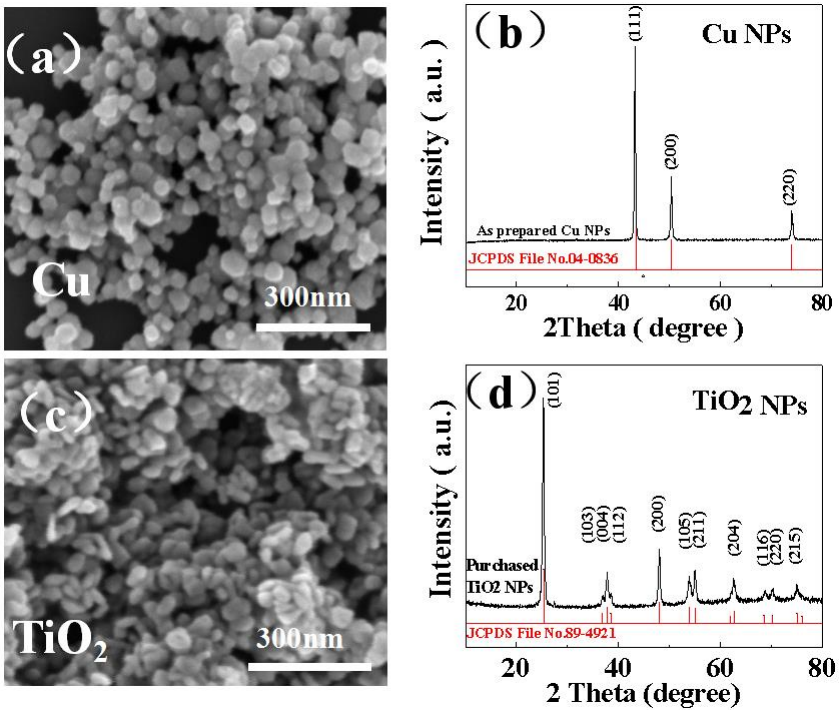

Fig. 2 SEM images of (a) Cu nanoparticles and (c) TiO_2 nanoparticles are shown in the picture. Similarly (b) XRD pattern of Cu nanoparticles and (d)TiO_2 nanoparticles are noted for characterization.

with the liquid solution saturated with Cu, the mechanism of screw dislocation driven growth of IMCs is pronounced and thus faceted planes appear at the surface of after-cooled Cu_6Sn_5 [9,14]. In addition to these observations, Sn + Cu NPs and Sn + TiO_2 NPs samples corresponding to Fig. 4(a2, a3), it is revealed that the nucleation of small Cu_6Sn_5 particles on their pre-existing IMC surface due to heterogeneous nucleation phenomena on the localized sites of nanoparticles [15]. Because of substantial increase in nucleation density of such smaller IMCs, it can be inferred that the thickness (H) of IMCs decrease with the addition of nanaoparticles. As shown in Fig. 6(a), the average thickness (H) of Cu_6Sn_5 is reduced for nanoparticles added solders (Sn + Cu NPs, Sn + TiO_2) with an increment in reflow duration. The decrease of H may be attributed to the suppression of IMC whiskers by nanoparticles as depicted in Fig. 3. Since, both nanoparticles suppress H more or less equally, the ratio of thickness is only compared between IMCs of Sn and Sn+ TiO_2 solders in Table 1. At reflow duration of 120 s, the average thickness of IMC in TiO_2 is reduced by 25 % as compared to pure Sn solders. In context of IMC grain width or rod diameter (w) for reflow of 60 s or greater (saturated solution), referring to Figs. 4(b1, c1, b2, c2, b3,c3) and graph of Fig. 6(b) , generally it can be inferred that w increases with an increase in isothermal reflow dura-

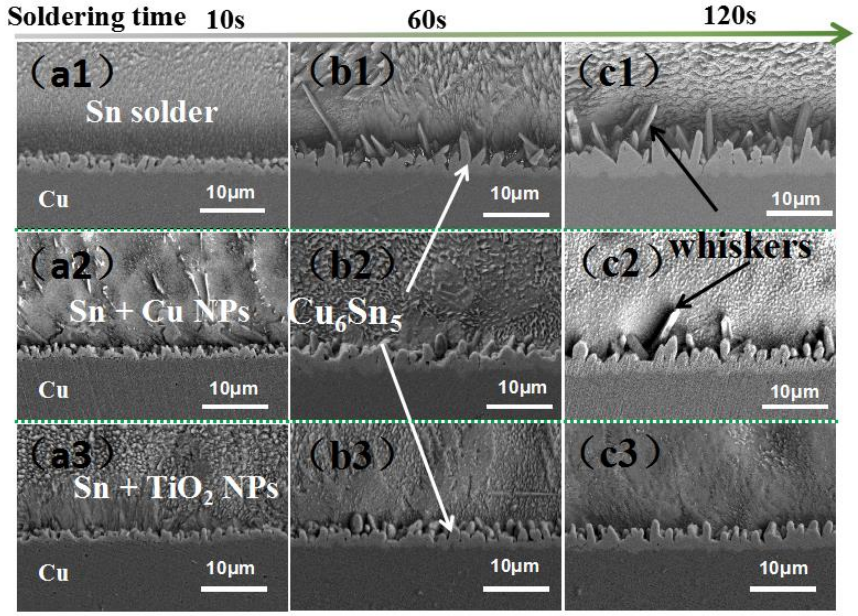

Fig. 3 The cross sectional images of (a1 - c1) Sn, (a2 - c2) Sn + Cu NPs and (a3 - c3) Sn +TiO_2 NPs as obtained from SEM.

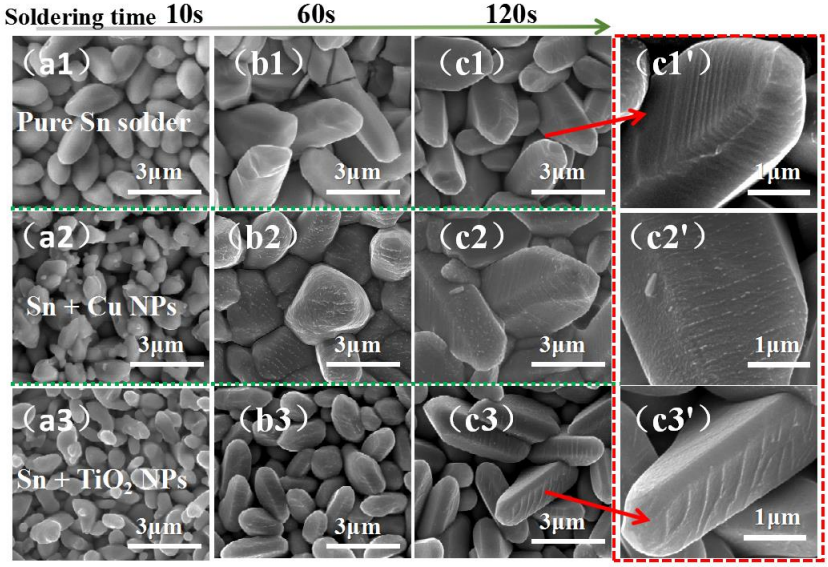

Fig. 4 The top-view images of (a1 - c1) Sn, (a2 - c2) Sn + Cu NPs and (a3 - c3) Sn +TiO_2 NPs show that IMC coarsen with an increment in reflow time. In the image, $c1'$, $c2'$ and $c3'$ show the magnified IMCs corresponding to c1, c2 and c3.

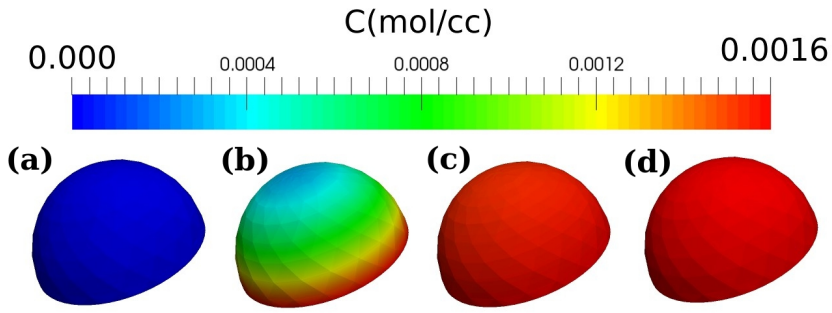

Fig. 5 Simulated values for Cu distribution in solder during reflow at 250 ℃ for t= (a) 0, (b) 10, (c) 60, and (d) 120 s.

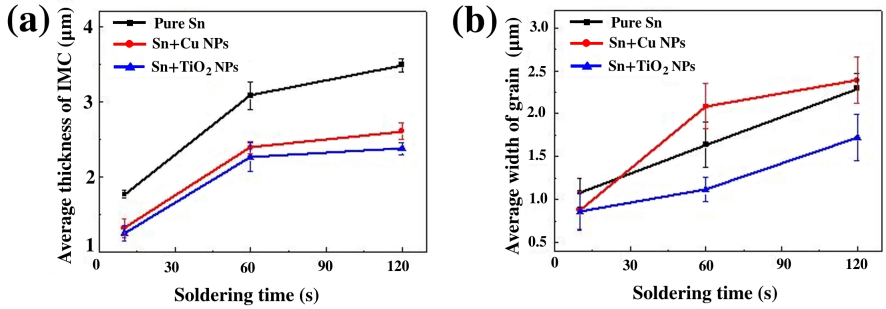

Fig. 6 For several solder types, the vertical thickness and lateral width of IMCs are provided in the graphical plots (a) and (b) respectively.

tion. However, it is noteworthy to mention that at greater reflow durations, the Cu_6Sn_5 grains/rods diameter of Sn + Cu NPs are larger than those of Sn solders whereas those of Sn + TiO_2 solders are significantly smaller as compared to pure Sn. As supported by the top view images of IMCs in Fig. 4(b2,c2), the presence of Cu nanoparticles promotes the annexation of smaller grains to larger diameter grains via the mechanism of Ostwald ripening. The IMC grain merging through Ostwald ripening mechanism is interrupted by non-metallic TiO_2 nanoparticles and thus result in the formation of Cu_6Sn_5 with small diameters and intra-grain spaces as shown in Fig. 4(b3,c3). As given in Table 1, the IMC grains in case of Sn + Cu NPs systems are 28 % larger than those for pure Sn samples at soldering reflow for 60 s and just bigger by 4 % at 120 s. On the other hand, Cu_6Sn_5 grains' width of Sn + TiO_2 solders are reduced or suppressed by 32 % as compared to pure Sn solder at 60 s and by 25 % at 120 s. It can be summarized that the IMC grain width enlargement by Cu NPs or suppression by TiO_2 nanoparticles is more pronounced for reflow duration of 60 s.

In general, the surface energy (γ) of the IMC, having Cu or TiO_2 nanoparticles adsorbed on its plane N, is reduced in accordance to the following ex-

Table 1 The change in height (H) and width (w) of IMC due to addition of nanoparticles are compared to that of pure solder.

Ratio \ Soldering time	10s	60s	120s
Thickness Ratio $H_{TiO_2}/H_{pure\ Sn}$	0.75	0.78	0.75
Width Ratio w_{Cu}/w_{Sn}	0.81	1.28	1.04
Width Ratio w_{TiO_2}/w_{Sn}	0.79	0.68	0.75

pression [16]:

$$\sum_N \gamma^N A_N = \sum_N (\gamma_0^N - RT \int_0^m \frac{\Gamma^N}{m} dm) A_N \tag{1}$$

where A_N is the area of plane N of Cu_6Sn_5, γ_0 (=0.055 J/m^2) is the surface energy per unit area between IMC and pure liquid Sn, Γ^N is the amount of adsorbed nanoparticles in the plane and m is the concentration of the nanoparticles. This surface property of nanoparticles containing IMC planes, affects the Ostwald ripening mechanism induced lateral growth of Cu_6Sn_5 compounds. The concentration (C(r)) of Cu on the surface of IMC at a radius R during reflow, that is responsible for the latter's growth via Ostwald ripening, is given by the following Gibbs-Thompson relation 2 as [17]:

$$C(r) = C_0 e^{\left(\frac{2\gamma\Omega}{r\overline{R}T}\right)} \tag{2}$$

where C_0 (=1.6×10^{-3} mol/cc) is the equilibrium concentration of Cu in liquid solder, γ is the interfacial energy per unit area between Cu_6Sn_5 (with NPs adsorbed) and molten solder, Ω (=1.18×10^{-4} m^3/mol) is the molar volume of Cu_6Sn_5, r is the radius of curvature of Cu_6Sn_5, T is the temperature, and $\overline{R}$ is the gas constant. For two interacting IMCs with different radii r_1 and r_2 as shown in Fig. 7, the Cu concentration gradient in the lateral direction ,can be expressed as follow:

$$\frac{dC(r)}{dr} = -\frac{2\gamma\Omega C_0}{\epsilon\overline{R}T}\left(\frac{1}{r_1} - \frac{1}{r_2}\right) \tag{3}$$

where ϵ means the average separation among interfacial grains. It is assumed that the IMC grains are nearly hemispherical during isothermal reflow and thus $w \approx 2r$. Considering the diffusion coefficient of Cu in liquid solder as D_s (=6.44×10^{-9} m^2/s) and the liquid solder density as ρ_l, the diffusion flux of Cu from smaller IMC grain (w_1) towards the larger one (w_2), is now given by Fick's first law [18],

$$J_R = -D_s\rho_l\frac{dC(r)}{dr} = -\frac{-2D_s\rho_l\Omega\gamma C_0}{\epsilon\overline{R}T}\left(\frac{2}{w_1} - \frac{2}{w_2}\right) \tag{4}$$

In Eq. 4, with lowered value of apparent interfacial energy or surface energy (γ) in context of IMC with TiO_2 nanoparticles, the equilibrium concentration

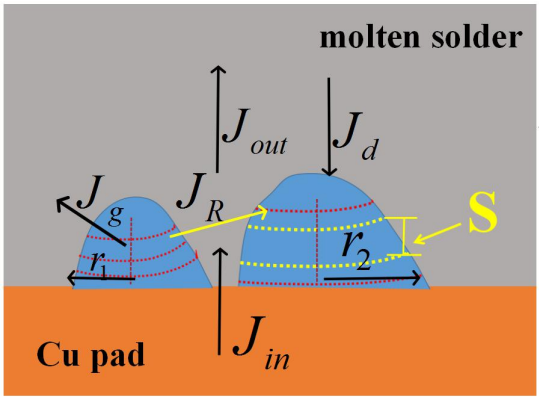

Fig. 7 The different forms of Cu flux responsible for Cu_6Sn_5 IMC evolution are schematically sketched in the figure and among them J_R is very significant when considering the Ostwald ripening mechanism..

C_0 at the vicinity of surface is also reduced by this inert particle and thus, the magnitude for J_{R,TiO_2} is suppressed correponding to reflow experiment of 60 s. So, the width of Cu_6Sn_5 grains in Sn + TiO_2 are smaller as compared to pure Sn solders. This is justified by the phase field simulation [19] of ostwald ripening based merging of a 0.1 μm sized IMC grain with a larger IMC of 0.5μm diameter, as presented in Fig. 8. With the use of non-dimensionalized time,diffusivity and interface energy; the time fractions (a1, a2), (b1,b2) and (c1, c2) represent 0, 0.5 and 1 respectively. The simulation results in Fig. 8(a2-c2), where diffusivity is reduced by an order of 1 and interfacial energy is reduced by 50 %; it is observed in the figure that the ripening mechanism is suppressed significantly . In the solders, the adsorption of inert TiO_2 on IMC surface, by acting as the barrier for diffusion flux of Cu between IMC and liquid solder in one hand whereas by reducing interfacial energy in the other hand, can in combined form retard the mobility of the coarsening mechanism between adjacent IMC grains as in Fig. 8(a2-c2) [20]. The role of TiO_2 nanoparticles in retarding the grain boundary diffusion between two IMCs remains as a topic of future study. As the reflow duration is increased, C_0 is of greater magnitude can slightly enhance the lateral flux of Cu. In context of Sn + Cu NPs solder system, the inhibitory effect of reduced γ on $J_{R,Cu}$ is counteracted by the amplified magnitude of C_0 supplied by the presence of Cu within the NPs. Thus, the resultant $J_{3R,Cu}$ is greater than $J_{R,undoped}$, thereby producing wider IMC grains in the Sn +Cu NPs solders for reflow duration of 60 s. And with the increase of reflow time, the difference in equilibrium concentration between Cu doped and undoped solders is lowered and thus the grain width are similar.

In the magnified SEM image of IMC of over-etched specimen as shown in Fig. 4($c1^{'}$), the spiral growth trajectory induced by screw-dislocation driven growth mechanism is observable. As shown in the figure the screw dislocation in Cu_6Sn_5 IMC is along the crystal direction [0 0 0 1]. For TiO_2 added solder

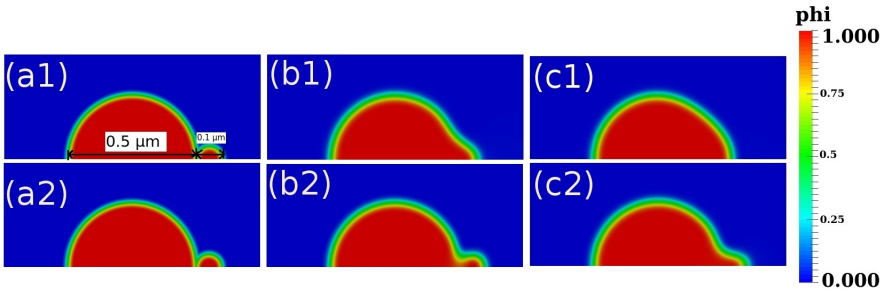

Fig. 8 For phase field analysis of ripening of two adjacent IMCs of different initial radii, the figures in the top half (a1-c1) correspond to unhindered mechanism whereas the images in bottom half (a2-c2) represent the retardation in radial growth owing to the reduction of mobility by order of 1.

system, as shown in Fig. 4($c3^{'}$), the helix angle made with the plane parallel to the basal plane of the IMC is greater than in context of that of pure Sn solder system. It is thus reasonable to assume that for an IMC with a given value of burgers vector for screw dislocation, the constraining of width by TiO_2 nanoparticles can lead to the greater helicity of the dislocation motion in Sn + TiO_2 samples. However, in Cu_6Sn_5 IMC rods , in context of Fig. 3($c2^{'}$)with lateral growth due to presence of Cu NPs, the helical angle is smaller. It is noteworthy to understand the Cu supply depletion rate in IMC growth due to the presence of suppressant nanoparticles such as TiO_2.

In general, the additions of nanoparticles(NPs) to the interface to the liquid Sn/ solid Cu interface can enhance the heterogeneous nucleation density of IMC , reduce the interfacial energy of IMC and influence the Cu concentration in the solder. These aspects determine the overall growth behavior of the intermetallic compounds. The enhancement in heterogeneous nucleation density of IMC triggered by reactive/inert NPs, can be correlated with an overall reduction in height or thickness of IMC layer. In case of metallic nanoparticles, having a tendency to undergo interfacial reaction , the effect on surface energy of IMC/solder is minimized once the NP dissolves or reacts with solder at vicinity of IMC and hence lateral or radial Ostwald ripening is promoted to cause a moderate increase in IMC width. For inert or non-reactive TiO_2 nanoparticles, the effect on interfacial energy remains effective permanently and lateral Ostwald ripening is retarded, thus rendering suppressed IMC width.

Thus, suppressant nanoparticles such as TiO_2 try to reduce the width of the IMC crystal by retarding the lateral flux J_R whereas the Cu nanoparticles produce the opposite effect. As noted in [1] , TiO_2 reinforced solder joints have a higher shear strength than the pure solder based joints. Since the reduction in width of IMC in Sn + TiO_2 solder systems is associated with the presence of interspaces between IMC grains, the liquid solder can flow into this space and therefor grip between IMC and solder becomes stronger. Hence, the shear strength of the solder joint is enhanced. Therefore, this research hopefully

may utilized in tailoring the morphology and grain size of Cu_6Sn_5 crystal, even property design of IMCs for electronic packaging industries.

4 Conclusions

In summary, the addition of TiO_2 nanoparticles has been observed to suppress both the heightwise thickness and radial width of the Cu_6Sn_5 IMC in Sn/Cu joints. On the other hand, Cu nanoparticles lead to the increase of the lateral size of the IMC although they suppress the heightwise thickness. The results have been analyzed using experimental and numerical results. The suppression of lateral growth of adjacent IMCs by TiO_2 addition results in the formation of gaps or spaces between IMC grains, which can be subsequently filled by liquid solder during the remaining soldering procedure. This can enhance the grip or bonding between solder and IMC , thereby enhancing the shear property of the resultant solder joints.

Acknowledgement

This work was supported by the National Natural Science Foundation of China (Grant Nos: 51571049 and 51675080), "Research Fund for International Young Scientists" of National Natural Science Foundation of China (Grant Number: 51750110504) and China Postdoctoral Science Foundation (Grant Number: 2017M611215).

References

1. M. A.A. Mohd Salleh, S. D. McDonald, C. M. Gourlay, H. Yasuda, and K. Nogita. Suppression of Cu6Sn5 in TiO2 reinforced solder joints after multiple reflow cycles. *Mater. Des.*, 108:418–428, 2016.
2. Fei Xing, Jia Yao, Jingwei Liang, and Xiaoming Qiu. Influence of intermetallic growth on the mechanical properties of Zn-Sn-Cu-Bi/Cu solder joints. *J. Alloys Compd.*, 649:1053–1059, 2015.
3. Fei Xing, Qinghui Shang, Yuzhen Lu, Jingwei Liang, and Xiaoming Qiu. Intermetallic compounds growth suppression in ZSCB solder with RE addition on Cu substrate. *J. Alloys Compd.*, 666:122–130, 2016.
4. Yilong Huang, Ziyang Xiu, Gaohui Wu, Yanhong Tian, Peng He, Xiaolong Gu, and Weimin Long. Improving shear strength of Sn-3.0Ag-0.5Cu/Cu joints and suppressing intermetallic compounds layer growth by adding graphene nanosheets. *Mater. Lett.*, 169:262–264, 2016.
5. G. K. Sujan, A. S M A Haseeb, and A. B M Afifi. Effects of metallic nanoparticle doped flux on the interfacial intermetallic compounds between lead-free solder ball and copper substrate. *Mater. Charact.*, 97:199–209, 2014.
6. S. Y. Chang, C. C. Jain, T. H. Chuang, L. P. Feng, and L. C. Tsao. Effect of addition of TiO2 nanoparticles on the microstructure, microhardness and interfacial reactions of Sn3.5AgXCu solder. *Mater. Des.*, 32(10):4720–4727, 2011.
7. L. Qu, N. Zhao, H. J. Zhao, M. L. Huang, and H. T. Ma. In situ study of the real-time growth behavior of Cu6Sn 5 at the Sn/Cu interface during the soldering reaction. *Scr. Mater.*, 72-73:43–46, 2014.

8. J W Xian, S A Belyakov, M Ollivier, K Nogita, H Yasuda, and C M Gourlay. Cu6Sn5 crystal growth mechanisms during solidification of electronic interconnections. *Acta Mater.*, 126:540–551, 2017.
9. Fei Meng, Stephen A. Morin, Audrey Forticaux, and Song Jin. Screw dislocation driven growth of nanomaterials. *Acc. Chem. Res.*, 46(7):1616–1626, 2013.
10. Xiangling Ren, Dong Chen, and Fangqiong Tang. Shape-Controlled Synthesis of Copper Colloids with a Simple Chemical Route. *J. Phys. Chem. B*, 109(33):15803–15807, aug 2005.
11. Shengyan Shang, Anil Kunwar, Yanfeng Wang, Xiao Qi, Haitao Ma, and Yunpeng Wang. Synthesis of Cu@Ag coreshell nanoparticles for characterization of thermal stability and electric resistivity. *Appl. Phys. A*, 124(7):492, jul 2018.
12. Natalie L. Gruenke, M. Fernanda Cardinal, Michael O. McAnally, Renee R. Frontiera, George C. Schatz, and Richard P. Van Duyne. Ultrafast and nonlinear surface-enhanced Raman spectroscopy. *Chem. Soc. Rev.*, 45(8):2263–2290, 2016.
13. G. K. Sujan, A. S M A Haseeb, Hiroshi Nishikawa, and M. A. Amalina. Interfacial reaction, ball shear strength and fracture surface analysis of lead-free solder joints prepared using cobalt nanoparticle doped flux. *J. Alloys Compd.*, 695(3):981–990, 2017.
14. Anil Kunwar, Bingfeng Guo, Shengyan Shang, Peter Råback, Yunpeng Wang, Jun Chen, Haitao Ma?b, Xueguan Song, and Ning Zhao. Roles of interfacial heat transfer and relative solder height on segregated growth behavior of intermetallic compounds in Sn/Cu joints during furnace cooling. *Intermetallics*, (In press), 2018.
15. A. S M A Haseeb, Y. M. Leong, and M. M. Arafat. In-situ alloying of Sn-3.5Ag solder during reflow through Zn nanoparticle addition and its effects on interfacial intermetallic layers. *Intermetallics*, 54:86–94, 2014.
16. Yi Li and Y.C. Chan. Effect of silver (Ag) nanoparticle size on the microstructure and mechanical properties of Sn58BiAg composite solders. *J. Alloys Compd.*, 645:566–576, 2015.
17. T. Küpper and N. Masbaum. Simulation of Particle Growth and Ostwald Ripening via the Cahn-Hilliard Equation. *Acta Metall. Mater.*, 42(6):1847–1858, 1994.
18. Yingxia Liu, Ying Ching Chu, and K. N. Tu. Scaling effect of interfacial reaction on intermetallic compound formation in Sn/Cu pillar down to 1μm diameter. *Acta Mater.*, 117:146–152, 2016.
19. Anil Kunwar, Michael R. Tonks, Shengyan Shang, Xueguan Song, Yunpeng Wang, and Haitao Ma. Quantitative polynomial free energy based phase field model for void motion and evolution in Sn under thermal gradient. In *2017 18th Int. Conf. Electron. Packag. Technol.*, pages 1502–1507. IEEE, aug 2017.
20. Sudipta Biswas, Daniel Schwen, and Vikas Tomar. Implementation of a phase field model for simulating evolution of two powder particles representing microstructural changes during sintering. *J. Mater. Sci.*, 2017.